Behavioral analysis of simultaneous photo-electro-catalytic degradation of antibiotic resistant *E. coli* and antibiotic via ZnO/CuI: A kinetic and mechanistic study

Extra supporting information

Model for inactivation of bacteria using photoelectrocatalysis-

Following reactions are involved in the inactivation mechanism of the microorganism via photoelectrocatalysis. The equations (A.1)-(A.17) are given below.

$$B(\text{Bacteria}) + V(\text{vacantsite}) \underset{k_{-ad1}}{\overset{k_{ad1}}{\rightleftharpoons}} B-C \quad \text{(A.1)}$$

$$H_2O + C \underset{k_{-ad2}}{\overset{k_{ad2}}{\rightleftharpoons}} C-H_2O \quad \text{(A.2)}$$

$$C + OH^- \underset{k_{-ad3}}{\overset{k_{ad3}}{\rightleftharpoons}} C-OH^- \quad \text{(A.3)}$$

$$CuO \xrightarrow{h\nu \geq \text{bandgap}(k_0)} h^+(\text{V.B.}) + e^-(\text{C.B.}) \quad \text{(A.4)}$$

$$C-OH^- + h^+ \underset{k_{-1}}{\overset{k_1}{\rightleftharpoons}} C-OH^\bullet \quad \text{(A.5)}$$

$$C-H_2O + h^+ \underset{k_{-2}}{\overset{k_2}{\rightleftharpoons}} C-OH^\bullet + H^+ \quad \text{(A.6)}$$

$$B-C + h^+ \xrightarrow{k_{h1}} \text{dead} \quad \text{(A.7)}$$

$$B + h^+ \xrightarrow{k_{h2}} \text{dead} \quad \text{(A.8)}$$

$$h^+(\text{V.B.}) + e^-(\text{C.B.}) \xrightarrow{k_r} \text{heat} \quad \text{(A.9)}$$

$$H_2O + \text{Electrode potential} \xrightarrow{k_{e1}} OH^\bullet + H^+ + e^- \quad \text{(A.10)}$$

$$OH^{\bullet} \xrightarrow{k_{e2}} \frac{1}{2}O_2 + H^+ + e^- \quad \text{(A.11)}$$

$$H_2O + e^- \xrightarrow{k_{e3}} \frac{1}{2}O_2 + OH^- \quad \text{(A.12)}$$

$$C + OH^{\bullet} \underset{k_{-ad4}}{\overset{k_{ad4}}{\rightleftharpoons}} C - OH^{\bullet} \quad \text{(A.13)}$$

$$[B-C] + [C-OH^{\bullet}] \xrightarrow{k_{S1}} [C] + [C-B-OH^{\bullet}]\,(\text{dead bacteria}) \quad \text{(A.14)}$$

$$[B] + [C-OH^{\bullet}] \xrightarrow{k_{S2}} [C] + [B-OH^{\bullet}]\,(\text{dead bacteria}) \quad \text{(A.15)}$$

$$[OH^{\bullet}] + [B-C] \xrightarrow{k_{S3}} [C] + [B-OH^{\bullet}]\,(\text{dead bacteria}) \quad \text{(A.16)}$$

$$[B] + [OH^{\bullet}] \xrightarrow{k_{S4}} [B-OH^{\bullet}]\,(\text{dead bacteria}) \quad \text{(A.17)}$$

Rate of disappearance of bacteria

$$-r_b = k_{h1}[B-C][h^+] + k_{h2}[B][h^+] + k_{S1}[B-C][C-OH^{\bullet}] + k_{S2}[B][C-OH^{\bullet}] + k_{S3}[B-C][OH^{\bullet}] + k_{S4}[B][OH^{\bullet}] \quad \text{(A.18)}$$

According to pseudo steady state approximation, the rate of generation of radicals, concentration of holes, electrons and adsorbed species can be considered zero, as given in equations (A.19)-(A.22).

$$\frac{d[OH^{\bullet}]}{dt} = 0 \quad \text{(A.19)}$$

$$\frac{d[h^+]}{dt} = 0 \quad \text{(A.20)}$$

$$\frac{d[e^-]}{dt} = 0 \quad \text{(A.21)}$$

$$\frac{d[B-C]}{dt} = 0 \quad \text{(A.22)}$$

Substitution of rate expression from the above mentioned reactions involved in inactivation mechanism (equations (A.1)-(A.17)) in (A.19)-(A.22) gives the following expressions (A.23)-(A.26).

$$-k_{S3}[B-C][OH^{\bullet}]-k_{S4}[B][OH^{\bullet}]+k_1[C-OH^-][h^+]+k_{-1}[C-OH^{\bullet}]+k_2[C-H_2O][h^+]- k_{-2}[C-OH^{\bullet}][H^+]-k_{S1}[B-C][C-OH^{\bullet}]-k_{S2}[B][C-OH^{\bullet}]+k_{e1}[H_2O]\lambda-k_{e2}[OH^{\bullet}]=0 \quad \text{(A.23)}$$

$$k_0\alpha[C]-k_1[C-OH^-][h^+]+k_{-1}[C-OH^{\bullet}]-k_2[C-H_2O][h^+] +k_{-2}[C-OH^{\bullet}][H^+]-k_r[h^+][e^-]=0 \quad \text{(A.24)}$$

$$k_0\alpha[C]-k_r[h^+][e^-]=0 \quad \text{(A.25)}$$

$$k_{ad1}[B][C]-k_{-ad1}[B-C]-k_{S1}[B-C][C-OH^{\bullet}]-k_{S3}[B][C-OH^{\bullet}]=0 \quad \text{(A.26)}$$

At equilibrium, adsorption will be equal to desorption. Rate expressions from equations (A.1) and (A.13) can be written as (A.27) and (A.28).

$$[B-C]=K_{ad1}[B][C] \quad \text{(A.27)}$$

$$[C-OH^{\bullet}]=K_{ad4}[C][OH^{\bullet}] \quad \text{(A.28)}$$

$$K_{ad4}=\frac{k_{ad4}}{k_{-ad4}},\ K_{ad1}=\frac{k_{ad1}}{k_{-ad1}}$$

Rate of disappearance of the microorganism after substituting values from (A.27) and (A.28)

$$-r_b=k_{h1}K_{ad1}[B][C][h^+]+k_{h2}[B][h^+]+k_{S1}K_{ad1}K_{ad4}[B][C]^2[OH^{\bullet}]+k_{S2}K_{ad4}[B][C][OH^{\bullet}] +k_{S3}K_{ad1}[B][C][OH^{\bullet}]+k_{S4}[B][OH^{\bullet}]$$

(A.29)

Rearranging (A.29)

$$-r_b=[h^+]\left(k_{h1}K_{ad1}[B][C]+k_{h2}[B]\right)+[OH^{\bullet}]\left(k_{S1}K_{ad1}K_{ad4}[B][C]^2+k_{S2}K_{ad4}[B][C]+k_{S3}K_{ad1}[B][C]+k_{S4}[B]\right) \quad \text{(A.30)}$$

Substituting the values from (A.27) and (A.28) to (A.23)-(A.26), we obtain the value of $[OH^{\bullet}]$

$$[OH^{\bullet}]=\frac{[h^+]\left\{k_1[C-OH^-]+k_2[C-H_2O]\right\}+k_{e1}[H_2O]\lambda}{k_{-1}K_{ad4}[C]+k_{-2}K_{ad4}[C][H^+]+k_{S1}K_{ad1}K_{ad4}[B][C]^2+k_{S2}K_{ad4}[B][C]+k_{S3}K_{ad1}[B][C]+k_{S4}[B]+k_{e2}} \quad \text{(A.31)}$$

Rearranging the terms in equation (S31) gives

$$[OH^{\bullet}] = \frac{[h^+]\left\{k_1[C-OH^-] + k_2[C-H_2O]\right\} + k_{e1}[H_2O]\lambda}{K_{ad4}[C]\left\{k_{-1} + k_{-2}[H^+] + k_{S1}K_{ad1}[B][C] + k_{S2}[B]\right\} + k_{S3}K_{ad1}[B][C] + k_{S4}[B] + k_{e2}} \quad \text{(A.32)}$$

Since, recombination is the fastest step and in $[h^+] = [e^-]$

The number of electrons excited from valence band will lead to the generation of equal number of holes. Therefore,

$$[h^+] = \sqrt{\frac{k_0\alpha[C]}{k_r}} \quad \text{(A.33)}$$

Substituting the value of $[h^+]$ from equation (A.33) to (A.32)

$$[OH^{\bullet}] = \frac{\sqrt{\frac{k_0\alpha[C]}{k_r}}\left\{k_1[C-OH^-] + k_2[C-H_2O]\right\} + k_{e1}[H_2O]\lambda}{K_{ad4}[C]\left\{k_{-1} + k_{-2}[H^+] + k_{S1}K_{ad1}[B][C] + k_{S2}[B]\right\} + k_{S3}K_{ad1}[B][C] + k_{S4}[B] + k_{e2}} \quad \text{(A.34)}$$

Substituting values from (A.33) and (A.34) to (A.30)

$$-r_b = [h^+]\left(k_{h1}K_{ad1}[B][C] + k_{h2}[B]\right) + [OH^{\bullet}]\left(k_{S1}K_{ad1}K_{ad4}[B][C]^2 + k_{S2}K_{ad4}[B][C] + k_{S3}K_{ad1}[B][C] + k_{S4}[B]\right) \quad \text{(A.35)}$$

$$-r_b = \left(\sqrt{\frac{k_0\alpha[C]}{k_r}}\right)\left(k_{h1}K_{ad1}[B][C] + k_{h2}[B]\right) + \left(\frac{\sqrt{\frac{k_0\alpha[C]}{k_r}}\left\{k_1[C-OH^-] + k_2[C-H_2O]\right\} + k_{e1}[H_2O]\lambda}{K_{ad4}[C]\left\{k_{-1} + k_{-2}[H^+] + k_{S1}K_{ad1}[B][C] + k_{S2}[B]\right\} + k_{S3}K_{ad1}[B][C] + k_{S4}[B] + k_{e2}}\right)\left(k_{S1}K_{ad1}K_{ad4}[B][C]^2 + k_{S2}K_{ad4}[B][C] + k_{S3}K_{ad1}[B][C] + k_{S4}[B]\right) \quad \text{(A.36)}$$

Terms from equation (A.36) are replaced by following generalized parameters given by k_a, k_b, k_c and k_h

$$k_a = \sqrt{\frac{k_0\alpha[C]}{k_r}}\left\{k_1[C-OH^-] + k_2[C-H_2O\right\} + k_{e1}[H_2O]\lambda \quad \text{(A.37)}$$

$$k_b = k_{S1}K_{ad1}K_{ad4}[C]^2 + k_{S2}K_{ad4}[C] + k_{S3}[C] + k_{S4} \quad \text{(A.38)}$$

$$k_c = K_{ad4}[C]\left(k_{-1} + k_{-2}[H^+]\right) + k_{e2} \quad \text{(A.39)}$$

$$k_h = \sqrt{\frac{k_0 \alpha [C]}{k_r}} \left[k_{h1} K_{ad1} [C] + k_{h2} \right] \tag{A.40}$$

In case of photoelectrocatalysis, the above parameter values of k_a, k_b, k_c, and k_h (A.37)-(A.40) are valid. After substitution of these parameters in equation (A.36), equation (A.41) is obtained as

$$-\frac{dB}{dt} = k_h [B] + \frac{k_a k_b [B]}{k_c + k_b [B]} \tag{A.41}$$

$$k_{abc} = \frac{k_a k_b}{k_c}, \; k_{bc} = \frac{k_b}{k_c}$$

Integrating equation (A.41),

$$\int_{B_0}^{B} \left(\frac{1 + k_{bc}[B]}{k_h [B] + k_h k_{bc} [B]^2 + k_{abc} [B]} \right) d[B] = -\int_0^t dt \tag{A.42}$$

$$t = -\int_{B_0}^{B} \left(\frac{1 + k_{bc}[B]}{[B]\left(k_h + k_{abc} + k_h k_{bc} [B]\right)} \right) d[B] \tag{A.43}$$

$$k_d = k_h + k_{abc}$$

$$t = -\int_{B_0}^{B} \left(\frac{1 + k_{bc}[B]}{[B]\left(k_d + k_h k_{bc} [B]\right)} \right) d[B] \tag{A.44}$$

Solution of equation (A.44) using partial fraction

$$-\int_{B_0}^{B} \left[\frac{1}{k_d [B]} + \frac{k_d k_{bc} - k_h k_{bc}}{k_d (k_d + k_h k_{bc} [B])} \right] d[B] = t \tag{A.45}$$

$$k_{dhbc} = \frac{k_d^2}{k_d k_{bc} - k_h k_{bc}}; \; k_{hd} = \frac{k_h k_d}{k_d - k_h}$$

$$-\left[\frac{1}{k_d} \ln \frac{[B]}{[B_0]} + \int_{B_0}^{B} \frac{1}{k_{dhbc} + k_{hd} [B]} d[B] \right] = t \tag{A.46}$$

$$-\left[\frac{1}{k_d}\ln\frac{[B]}{[B_0]}+\frac{1}{k_{hd}}\ln\left(\frac{k_{dhbc}+k_{hd}[B]}{k_{dhbc}+k_{hd}[B_0]}\right)\right]=t \qquad \text{(A.47)}$$

$$\ln\left[\left(\frac{[B_0]}{[B]}\right)^{(1/k_d)}\left(\frac{1+\frac{k_{hd}}{k_{dhbc}}[B_0]}{1+\frac{k_{hd}}{k_{dhbc}}[B]}\right)^{(1/k_{hd})}\right]=t \qquad \text{(A.48)}$$

In case of photocatalysis due to elimination of electrolytic pathway ((A.10)-(A.12)) k_{e1}, k_{e2} are equal to zero. Therefore, k_a and k_b can be rewritten as

$$k_a=\sqrt{\frac{k_0\alpha[C]}{k_r}}\left\{k_1[C-OH^-]+k_2[C-H_2O\right\}$$

$$k_c=K_{ad4}[C]\left(k_{-1}+k_{-2}[H^+]\right)$$

Equation (A.49) is obtained by substituting these above mentioned parameters in equation (A.36)

$$-\frac{d[B]}{dt}=k_h[B]+\frac{k_a k_b[B]}{k_c+k_b[B]} \qquad \text{(A.49)}$$

$$\ln\left[\left(\frac{[B_0]}{[B]}\right)^{\frac{1}{k_d}}\left(\frac{1+\frac{k_{hd}}{k_{dhbc}}[B_0]}{1+\frac{k_{hd}}{k_{dhbc}}[B]}\right)^{\frac{1}{k_{hd}}}\right]=t \qquad \text{(A.50)}$$

In case of electrolysis, the interaction steps of catalyst with bacteria and generation of charge carriers and recombination, direct hole attack can be omitted with k_h, k_1, k_0, k_r k_2, k_{-1}, k_{-2}, k_{S1}, k_{S2}, k_{S3}, K_{ad1}, K_{ad4} values to be equal to zero. Parameters (A.37)-(A.40) can be rewritten as the expressions given below.

$$k_a=k_{e1}[H_2O]\lambda;\ k_b=k_{S4};k_c=k_{e2}$$

Substitution of theses parameters in equation (A.36) gives equation (A.51)

$$-\frac{d[B]}{dt}=\frac{k_a k_b[B]}{k_c+k_b[B]} \tag{A.51}$$

$$k_{bc}=\frac{k_b}{k_c};\ k_d=k_{abc}$$

Integration of equation (A.51) gives equation (A.52)

$$\frac{1}{k_d}\ln\left[\frac{[B_0]}{[B]}\right]+\frac{k_{bc}}{k_d}\left([B_0]-[B]\right)=t \tag{A.52}$$

In case of electrocatalysis charge carrier generation, recombination and direct hole attacks steps will be eliminated with k_h, k_1,k_{-1}, k_2, k_{-2}, k_0, k_r values equal to zero. Parameters k_a and k_c can be rewritten as expressions given below

$$k_a=k_{e1}[H_2O]\lambda;\ k_c=k_{e2}$$

Substitution of these parameters in equation (A.36) gives equation (A.53)

$$-\frac{d[B]}{dt}=\frac{k_a k_b[B]}{k_c+k_b[B]} \tag{A.53}$$

$$k_{bc}=\frac{k_b}{k_c};\ k_d=k_{abc}$$

Integration of equation (A.53) gives equation (A.54)

$$\frac{1}{k_d}\ln\left(\frac{[B_0]}{[B]}\right)+\frac{k_{bc}}{k_d}\left([B_0]-[B]\right)=t \tag{A.54}$$

X-ray photoelectron spectroscopy (after reaction)

XPS spectra of the elements O-1s, Cu-2p, I-3d and Zn-2p after the 8 h of reaction of the photocatalyst is shown in the figure A.1. In figure A.1 (d) shows the XPS spectrum of Cu-2p, a weak satellite peak at around 945 eV show the small amount of Cu2+ formation. Due to the leaching of Cu from the composite after successive 8 runs, the peaks intensity is not prominent as shown in the XPS before reaction. Similarly, Zn-2p peaks are prominent after the reaction due to the unmasking of CuI from ZnO, due to

photo corrosion during the reaction. Therefore, it can be said that CuI cannot be used as a photostable catalyst.

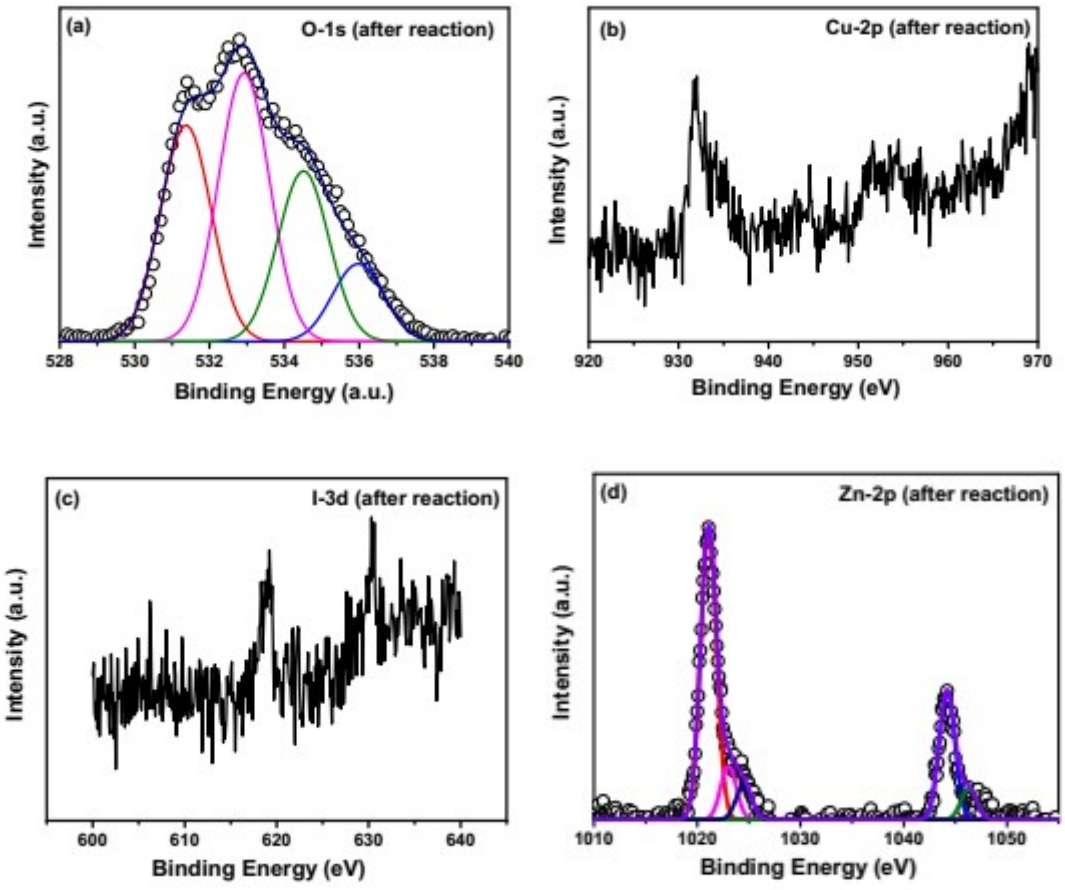

Figure A.1 XPS spectra of ZnO/CuI composite after 8 h of reaction (a) C-1s (b) O-1s (c) Cu-2p (d) I-3d (e) Zn-2p

Bacterial inactivation SEM images-

Figure A.2 shows the SEM images of the working electrode after the reaction. The placement of bacteria all over the slides indicate why the activity in later runs must have reduced. The placement of bacteria reduces the present active sites on the slides that reduces the surface interaction of catalyst and the bacteria. Therefore, washing of the electrode is important with highly non-polar solvent such as DMSO. That can remove the bound bacterial cells from the catalysts. It has high affinity towards phospholipids.

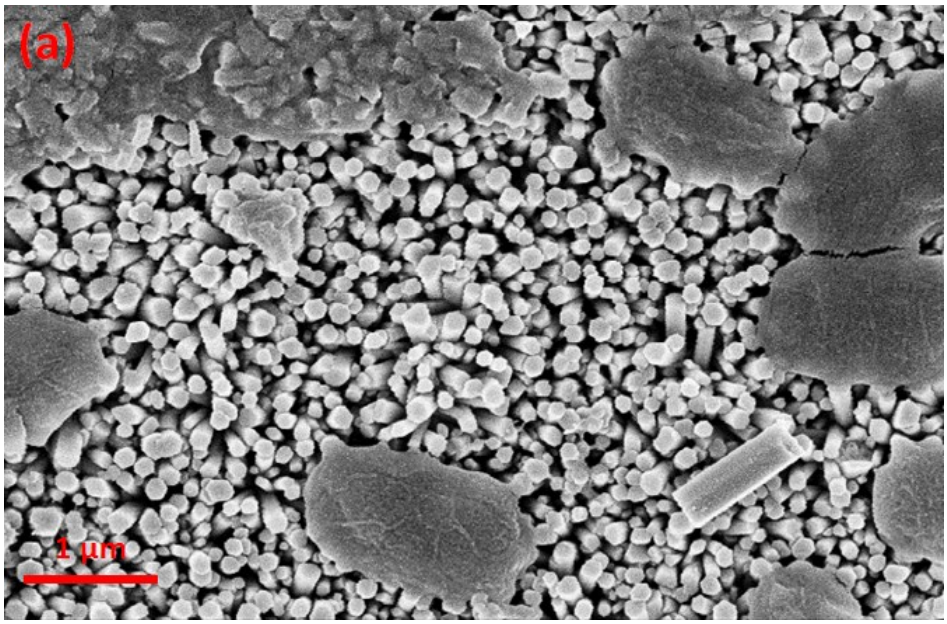
(a)
1 µm

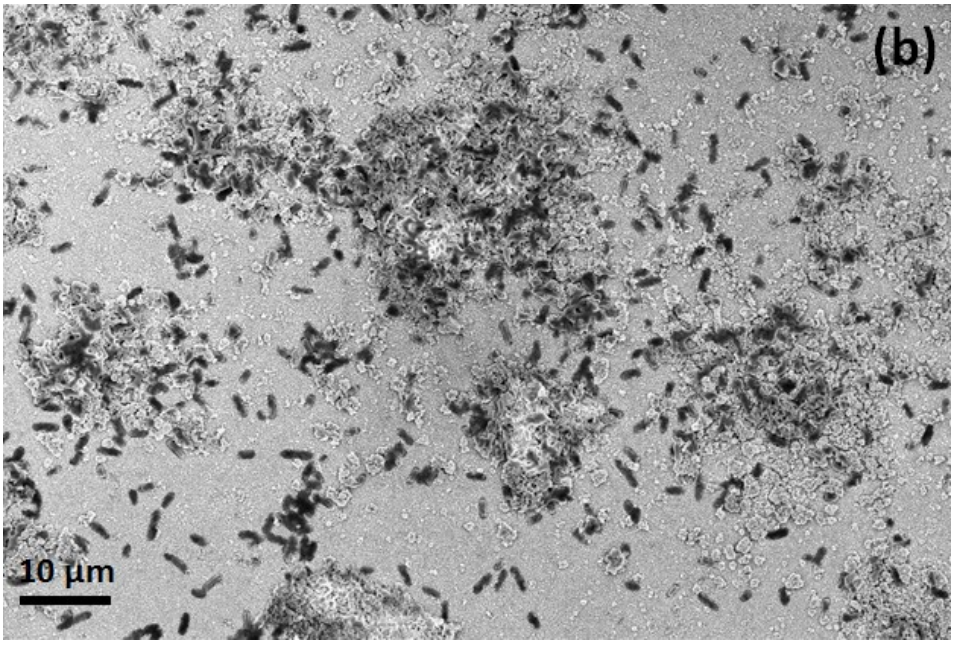
(b)
10 µm

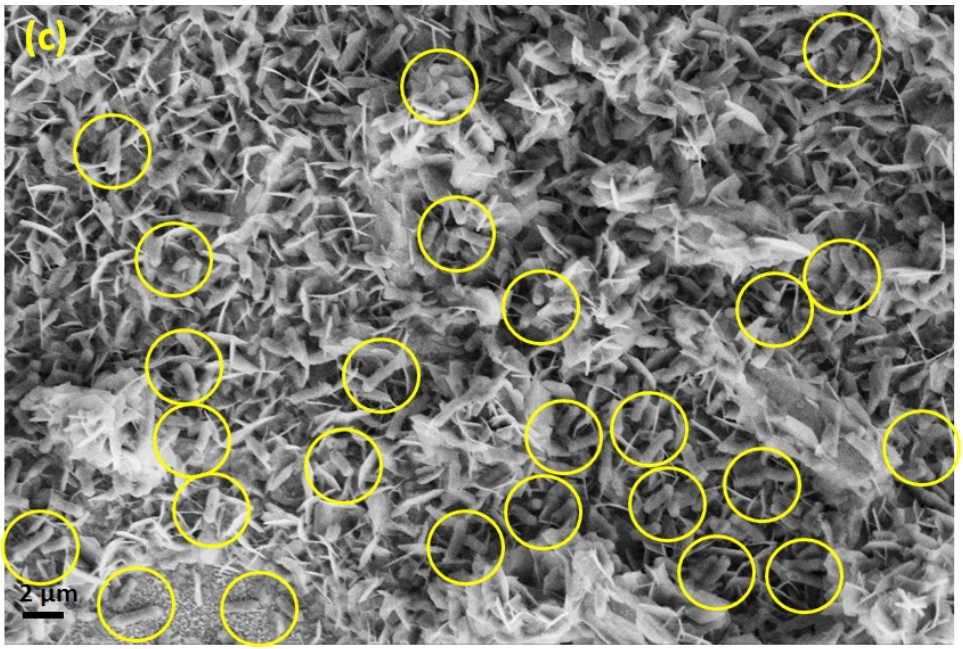

Figure A.2 SEM images of the FTO glass slide after the reaction (a) ZnO nanorods, (b & c) ZnO/CuI

Fourier transform infrared spectroscopy of bacterial cells –

Figure A.3 shows the FTIR spectra of bacterial calls drop casted on KBr pellet to detect the structural changes in the cells after 1 h exposure during photocatalysis. Humps indicated in the figure appeared in the live cells were disappeared in the spectra after 1 h of reaction. This clearly indicates that during the photocatalysis, the membrane of the cells is losing its integrity. Details of the bonds appearing and disappearing are described well in the literature [1].

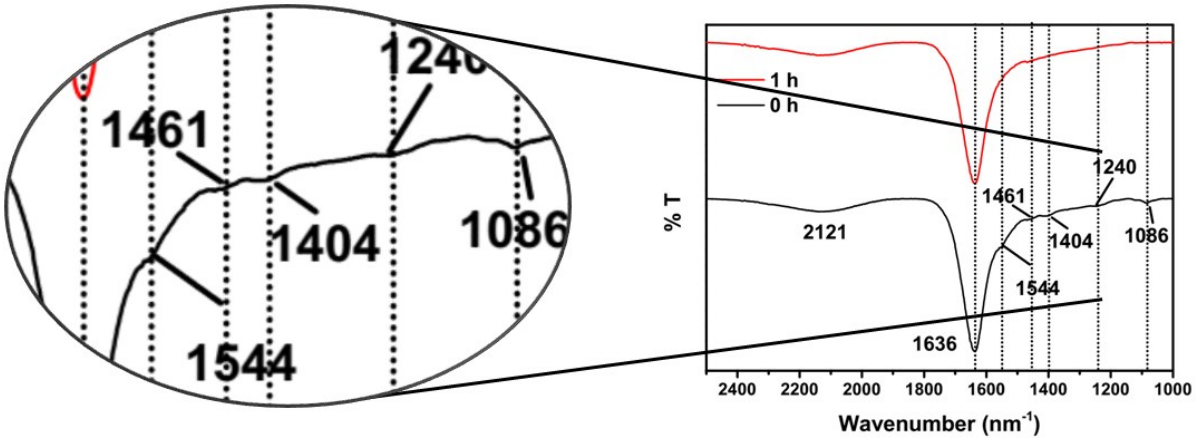

Figure A.3 FTIR spectra of *E. coli* before and after1 h of reaction

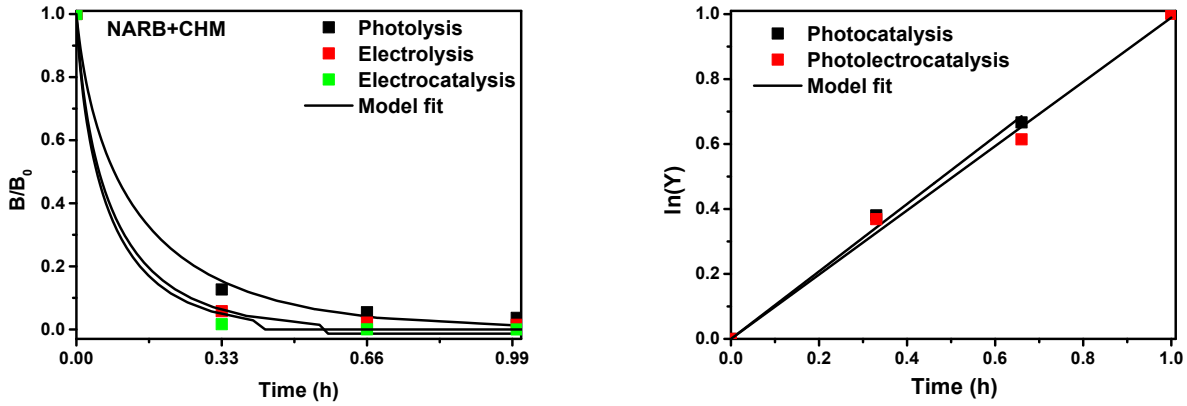

A.4 Kinetic fitting plots of NARB in NARB+CHM

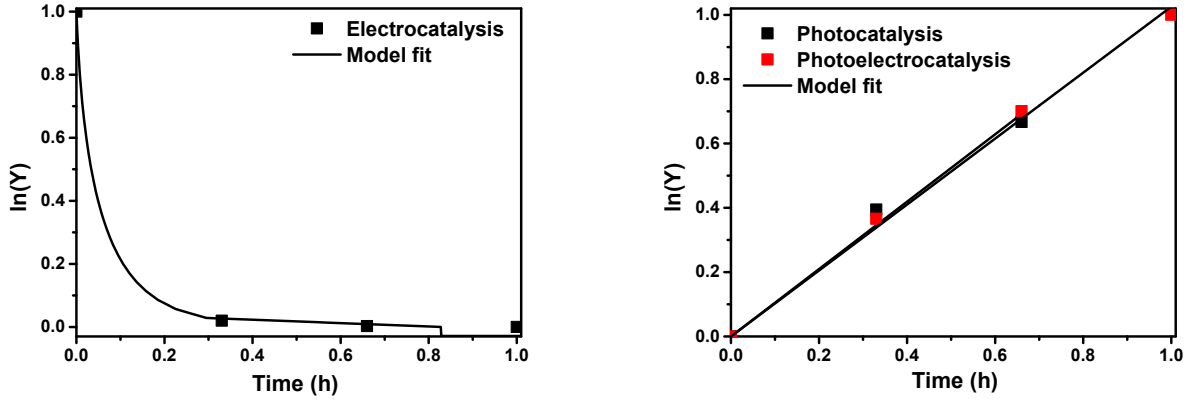

A.5 Kinetic fitting plots of ARB in ARB+CHM

Photocatalysis with powder catalysts (0.25 mg/L)-

The photocatalysis experiments were carried out for the composites prepared in powder form in the same ratio as obtained by ICP-MS analysis for immobilized catalyst i.e. 85:55 wt. ratio. It was found that the dark experiments show ~2-log reduction indicating leaching of the Cu ions from the composites. However, the dark reaction via ZnO/CuI composites show lower inactivation as shown in figure A.7.

Effect of CuI loading on ZnO-

Effect of CuI loading on ZnO was observed and shown in the figure A.7. Inactivation in absence of light showed less than 1 order difference for the coated (10, 20, 30 and 40 cycles)

CuI. Inactivation was almost similar due to the exposed surface area of the catalyst. However, photocatalysis for 30 cycles shows ~6 log reduction in 1 h which was higher than the 10, 20 and 40 cycles loading of CuI. Reduction in the inactivation for 40 cycles may be due to the lower penetration of light to the junction leading to the activation of electrons only through CuI.

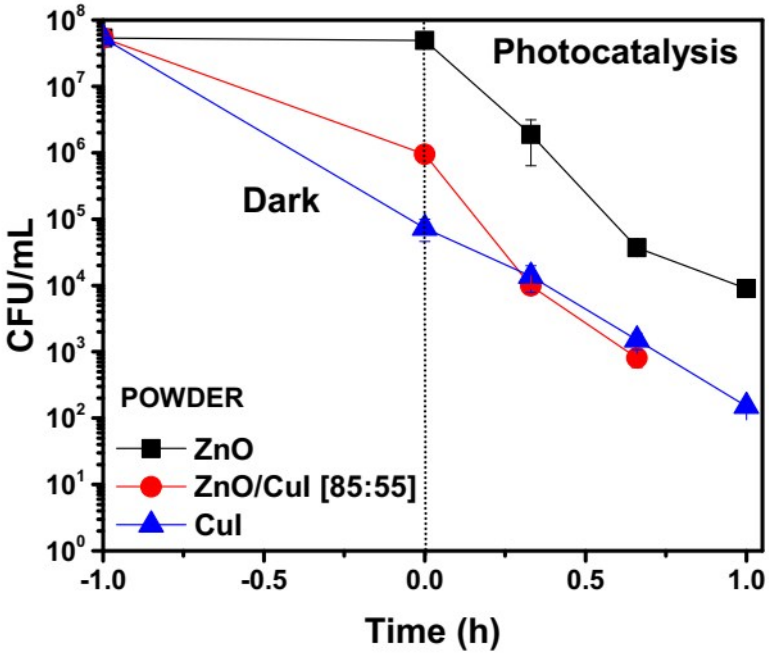

A.6 Inactivation using powder catalysts with initial concentration ~5×10^7 CFU/mL and catalyst loading 0.25 mg/L

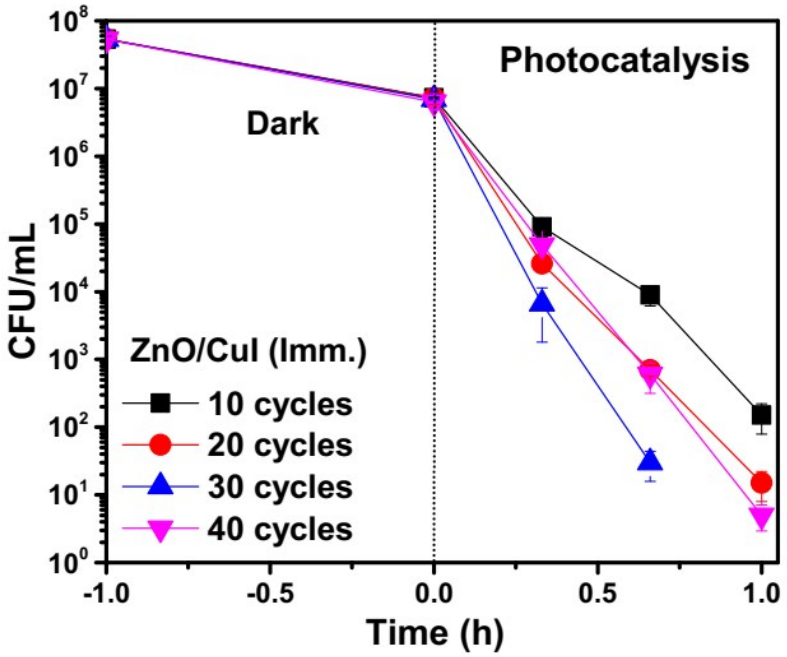

A.7 Effect of loading of CuI on immobilized ZnO ~5×10^7 CFU/mL

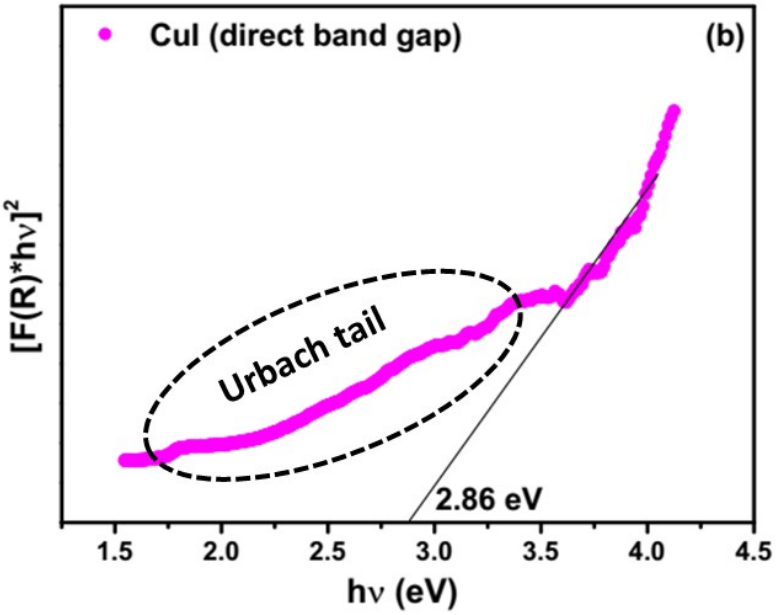

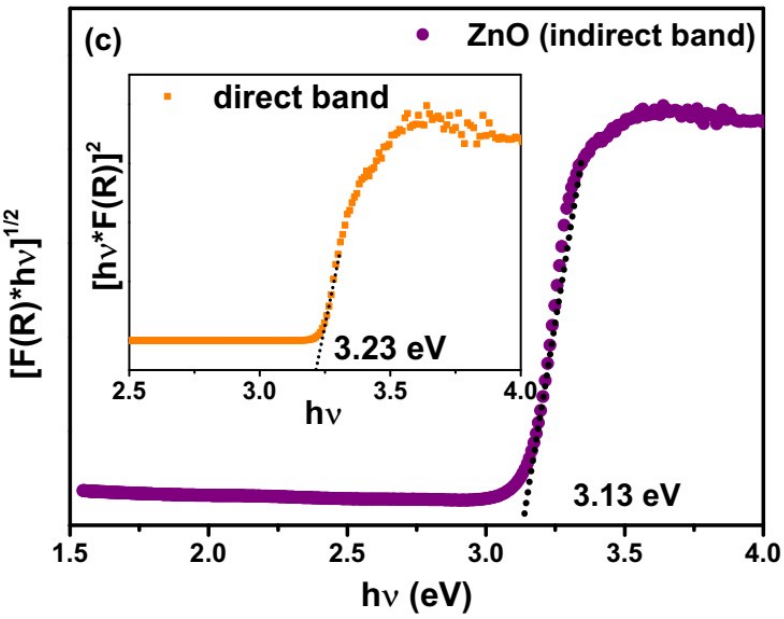

Figure A.8 (b) CuI (c) ZnO (indirect band), inset Tauc plot of ZnO with direct band gap

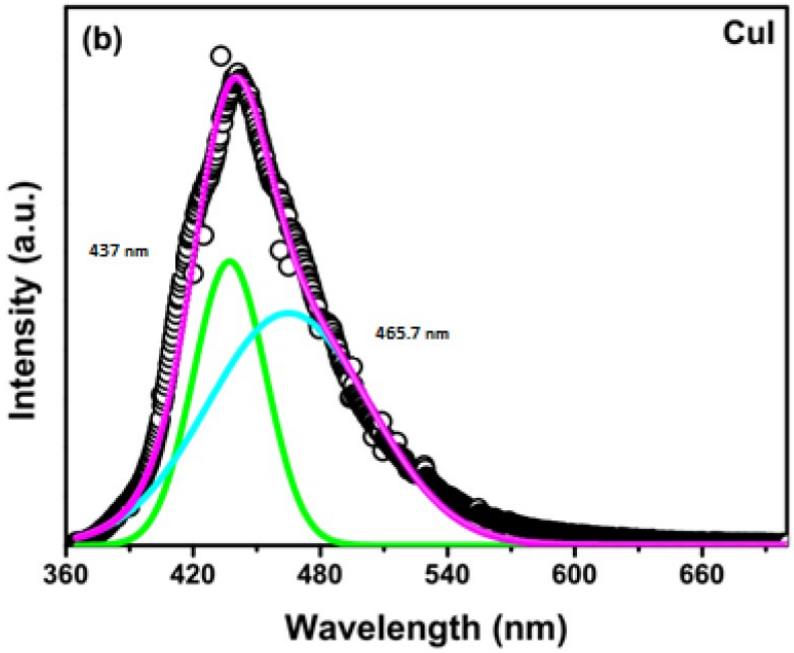

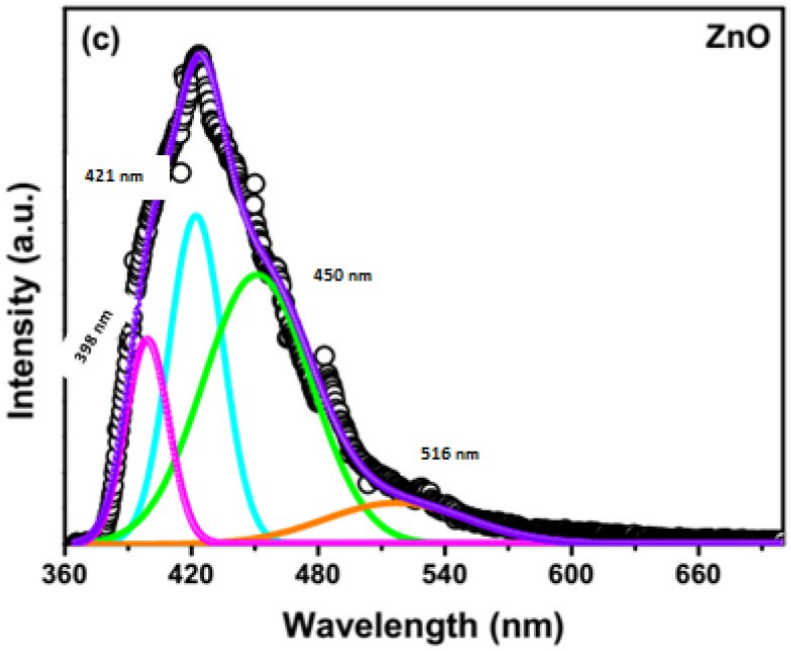

Figure A.9. Deconvoluted PL spectra of (b) CuI and (c) ZnO

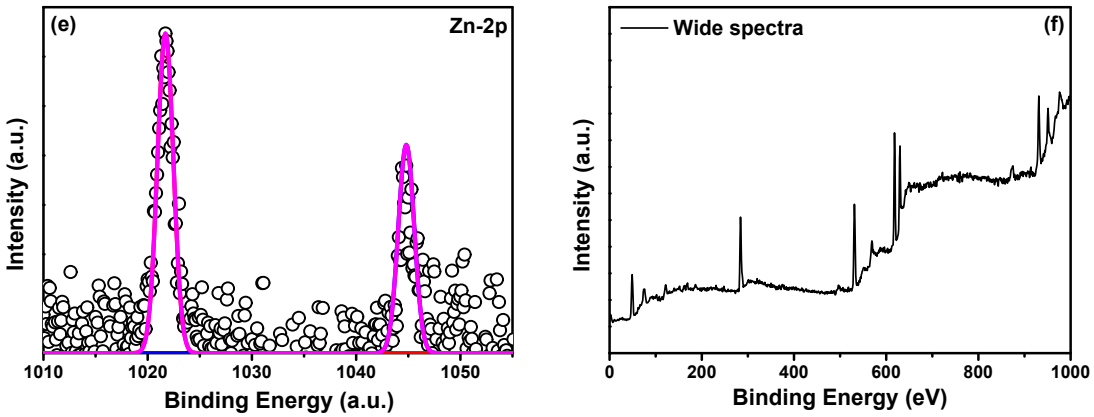

Figure A.10. XPS spectra of (e) Zn-2p and (f) wide spectra in the composite ZnO/CuI

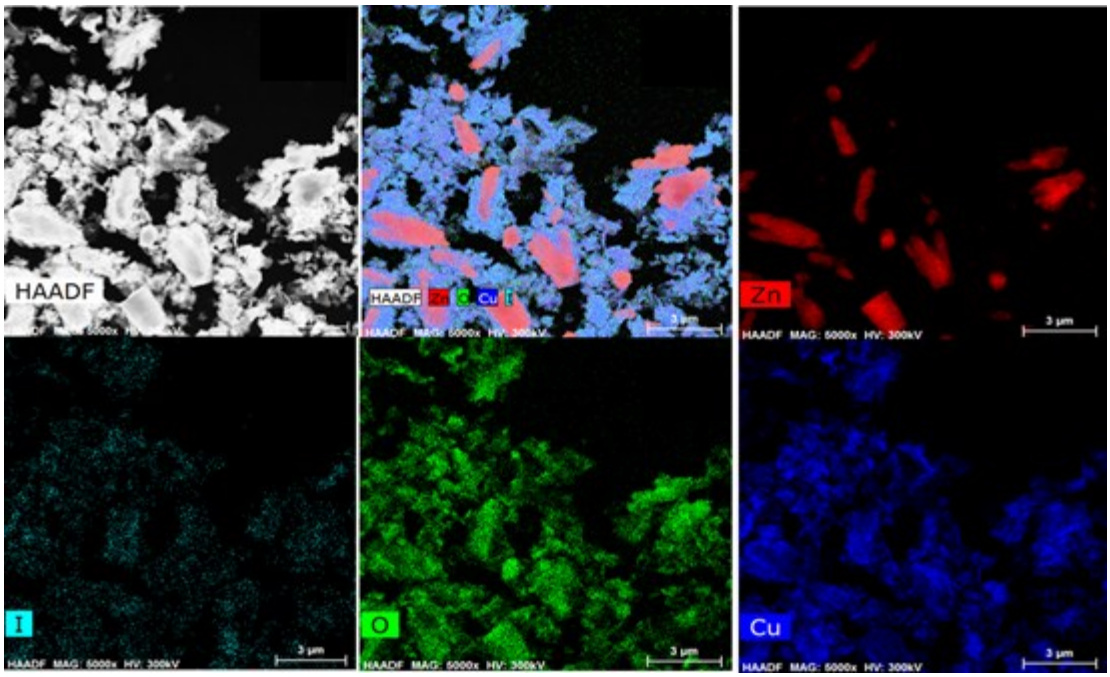

Figure A.11. SEAD images of elements of ZnO/CuI composite

ζ potential of the photocatalysts and bacteria-

Surface charge of a species plays a very crucial role in the analysis of electrostatic properties of the particle. Attraction and repulsion of two particles are strongly dependent on the surface charge of the particles. Therefore, zeta potential was carried out for the chloramphenicol, non-antibiotic resistant, antibiotic resistant bacterial strains of *E. coli* and the catalysts. The zeta potential values are mentioned in the Table 1.

All the particles or species possess negative charges with varying magnitude. Varying the pH of the solution may exhibit an opposite surface charge of the particle. However, the sustainability of bacteria in varying pH is also a challenge. Osmotic imbalance due to variation in pH is the well-known cause of cell death. Therefore, all the experiments were carried out for pH≈ 6.8-7. However, a good photocatalytic activity was achieved due to the freely suspended radicals. Therefore, it can be said that the zero-point charge of all the species are < 6.8.

Table A.1. Zeta potential of different species

Species	Zeta potential (mV)
Chloramphenicol	-18.48±1.27
NARB	-30.16±0.88
ARB	-0.47±.04
ZnO	-5.95±0.79
CuI	-1.56±0.16
ZnO/CuI	-5.76±0.27

Table A.2. Rate constants of photolysis, electrolysis, electrocatalysis, photocatalysis and photoelectrocatalytic reactions for bacterial inactivation

Experiments	Catalysts		k_h [min^{-1}]	k_{bc} [$CFU/mL]^{-1}$ [10^{-7}]	k_d [min^{-1}]
Electrolysis	**FTO**	**1 V**	0	1.0	1.37±0.05
EC	**ZnO .025 M**	**1V**	0	1.0	3.93±0.26
	CuI	**1V**	0	1.0	4.60±0.08
	ZnO /CuI	**1V**	0	1.0	9.77
Photolysis			0	1.0	1.05±0.06
PC	**ZnO NR**	**0.01 M**	3.67	15.79	5.80
		.025M	4.09	16.96	6.94
		0.05 M	4.44	18.04	8.01
		0.1 M	4.62	18.63	8.61
	CuI		3.75	16.00	6.00
	ZnO /CuI		6.31	27.12	17.14
	FTO	**1V**	3.15	14.63	4.61

PEC	**ZnO NR**	**1V**	4.19	17.27	7.24
	CuI	**1V**	5.36	21.60	11.58
	ZnO /CuI	**1V**	7.31	37.28	27.30

Table A.3. Rate constants of photolysis, electrolysis, electrocatalysis, photocatalysis and photoelectrocatalytic reactions for chloramphenicol degradation

Experiments	**Catalysts**			k_h [min^{-1}]	k_{bc} [CFU/mL]$^{-1}$	k_d [min^{-1}]
Electrolysis	**FTO**		**1 V**	0	0.26	0.075±0.005
EC	**ZnO**	**0.025 M**	**1V**	0	0.26	0.111±0.006
	CuI		**1V**	0	0.26	0.130±0.002
	ZnO NR/CuI		**1V**	0	0.26	0.168±0.001
Photolysis				0	0.26	0.140±0.013
PC	**ZnO NR**		**.025M**	0	0.26	0.275±0.011
	CuI			0	0.26	0.292±0.017
	ZnO NR/CuI			0	0.26	0.349±0.006
PEC	**FTO**		**1V**	0	0.26	0.094±0.005
	ZnO NR		**1V**	0	0.26	0.135±0.002
	CuI		**1V**	0	0.26	0.161±0.005
	ZnO NR/CuI		**1V**	0	0.26	0.215±0.011

Table A.4. Rate constants of the simultaneous degradation of E. coli (for non-antibiotic resistant strain) with antibiotics chloramphenicol

Catalysts [ZnO/CuI]	**Experiments**	k_h [min^{-1}]	k_{bc} [CFU/mL]$^{-1}$	k_d [min^{-1}]
Non antibiotic resistant bacteria (40 ppm)	**Photolysis**	0	1.00×10^{-7}	1.20±0.09
	Electrolysis	0	1.00×10^{-7}	2.05±0.19

	EC	0	1.00×10^{-7}	9.45±0.06
	PC	5.86	24.16×10^{-7}	14.18
	PEC	7.38	38.19×10^{-7}	28.20
Chloramphenicol (40 ppm)	**Electrolysis**	0	0.26	0.033
	Photolysis	0	0.26	0.040±0.002
	Photoelectrolysis	0	0.26	0.068±0.003
	EC	0	0.26	0.053±0.006
	PC	0	0.26	0.048±0.004
	PEC	0	0.26	0.084±0.005

Table A.5. Rate constants of the simultaneous degradation of *E. coli* (for antibiotic resistant strain) with antibiotics chloramphenicol

Type of bacteria	**Processes**	k_h **[min^{-1}]**	k_{bc} **[CFU/mL]$^{-1}$**	k_d **[min^{-1}]**
Antibiotic resistant bacteria (40 ppm)	**EC**	0	1.00×10^{-7}	7.93±0.75
	PC	5.44	21.93×10^{-7}	11.94
	PEC	6.53	27.46×10^{-7}	18.83
Chloramphenicol (40 ppm)	**Electrolysis**	0	0.26	0.038±0.001
	Photolysis	0	0.26	0.055±0.005
	Photoelectrolysis	0	0.26	0.126±0.005
	EC	0	0.26	0.117±0.010
	PC	0	0.26	0.125±0.006
	PEC	0	0.26	0.140±0.004

Growth mechanism

Nanorods- ZnO wurtzite structure is composed of tetrahedrally coordinated Zn^{2+} and O^{2-} present at alternating sides of c-axis. In ZnO, basal plane is a highly energetic and polar surface in comparison to other planes [57]. Therefore, these planes have growth rate lower than the plane with high energy and tend to maximize the areas and form the facets. One vertical side of the basal plane ends with the positively Zn^{2+} sites while other side ends with the negatively O^{2-} sites. The dipole is created between the two surfaces generated by these oppositely charged surfaces. This leads to the difference in the surface energy. Therefore, a stable structure of ZnO is generated by the formation of the polar facets [57, 58].

Synthesis of ZnO nanorods was achieved by using equimolar concentration of hexamine. Hexamine is a non-polar chelating agent and highly water soluble. Thermal decomposition of hexamine generates the massive release of hydroxyl ions. The non-polar behaviour of hexamine leads its binding to the non-polar facets (surfaces) of the ZnO morphology and gives rise to the epitaxial growth in one direction [57, 59]. However, in this case, the placement of the FTO slide at 45 degree facilitates the growth in random directions. As suggested by Jeon et al., the vertical rods grown in one direction showed lesser photocatalytic activity than the rods grown in multi-directions [60].

Roza et. al. performed studies by varying the concentration of hexamine with respect to the zinc precursor and observed relatively high nucleation rate to generate a high amount of ZnO nuclei. At higher molar ratios of hexamine, uneven growth of rods was observed [59].

Schematic 18 (a) shows the diagrammatic representation of sequential processes to synthesise ZnO/CuI composite as described in the experimental section.

SILAR- SILAR method consists of three major processes- (1) adsorption of the cations from the cationic precursor solution, (2) rinsing of the substrate with DI water for removal of weakly adsorbed cations and (3) reaction of anions with adsorbed cations. In our case, $CuSO_4$ was used as the cationic precursor [61]. However, the presence of Cu ions in +2 oxidation state in the precursor requires the need to reduce Cu from +2 to +1 oxidation state. Therefore, equimolar sodium thiosulphate was added to reduce Cu from +2 to +1 oxidation state and form a complex due to the presence of thiosulphate ligand $(S_2O_3)^{2-}$ for easy adsorption of the Cu ions at the substrate [62, 63].

Better understanding of the SILAR deposition of CuI can be understood by given reactions. 0.1 M solution of $CuSO_4$ and 0.1 M $Na_2S_2O_3$ and 0.025 M KI solution was prepared. Schematic A.11 (b) shows the schematic of the SILAR method [62, 64].

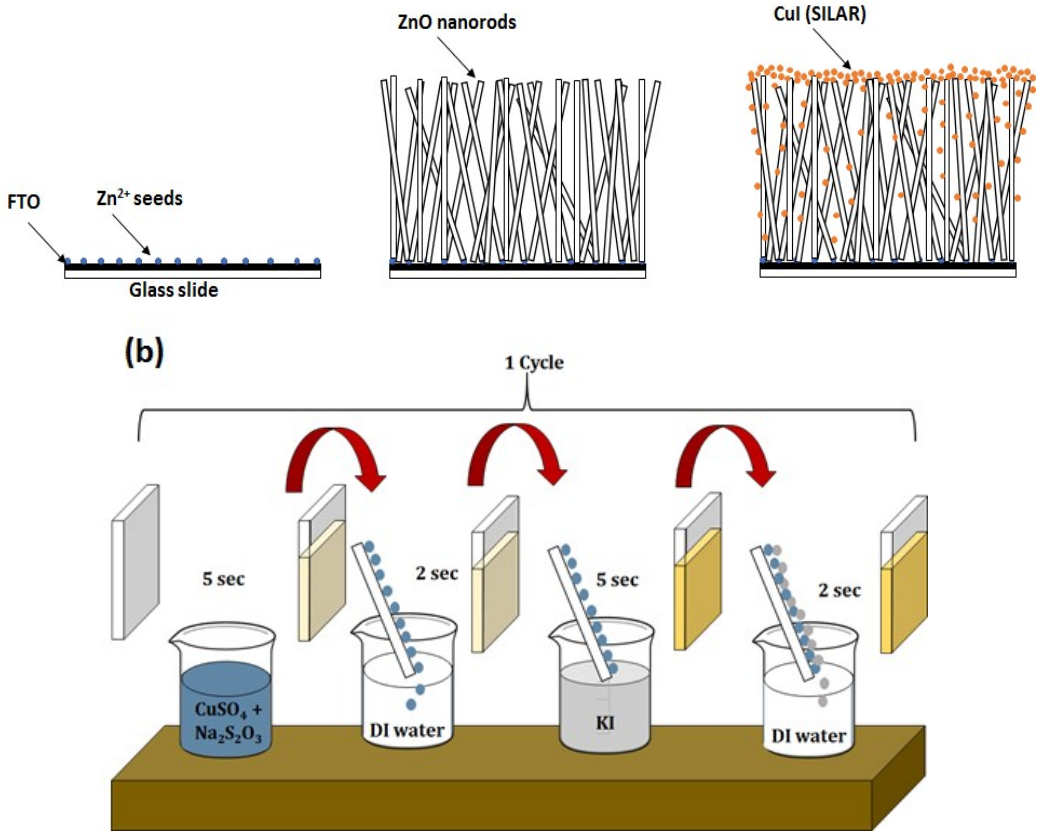

Figure A.11. Schematic of (a) Catalyst composite formation, (b) SILAR method

References

[1] C. Hu, J. Guo, J. Qu, X. Hu, Photocatalytic degradation of pathogenic bacteria with AgI/TiO2 under visible light irradiation, Langmuir 23 (2007) 4982-4987.